The Open Biotechnology Journal
DOI: 10.2174/0118740707325368240722062451, 2024, 18, e18740707325368
ISSN: 1874-0707
1

RESEARCH ARTICLE **OPEN ACCESS**

Terminalia Arjuna (Roxb.) Wight & amp; Arn: Unveiling its Potential as a Mosquito Control Agent through Biosynthesized Nanomaterials and Computational Analysis against *Aedes Aegypti* and *Aedes Albopictus*

B Padmavathy[1], B Samuel Ebinezer[1], K Karthikeyan[2], M Arumugam[3], M Ayyanar[4], S Padma Priya[5], S Amalraj[6], S Prabhu[6,*] and S Antony Ceasar[6,7,*]

[1]*Department of Physics, Government Arts College (Autonomous), Kumbakonam-612002, Affiliated to Bharathidasan University, Tiruchirappalli, India*
[2]*Department of Botany, Government Arts College (Autonomous), Kumbakonam-612002, Affiliated with Bharathidasan University, Tiruchirappalli, India*
[3]*Department of Botany, J.J. College of Arts and Science (Autonomous), Pudukkottai 622422, Affiliated with Bharathidasan University, Tiruchirappalli, India*
[4]*PG and Research Department of Botany, AVVM Sri Pushpam College (Autonomous) Poondi, (Affili-ated to Bharathidasan University), Thanjavur (Dist), 613 503, Tamil Nadu, India*
[5]*Oral Biology and Oral Pathology, RAK College of Dental Sciences, RAK Medical & Health Sciences University, Ras Al Khaimah, UAE*
[6]*Division of Phytochemistry and Drug Design, Department of Biosciences, Rajagiri College of Social Sciences, Cochin, 683 104, Kerala, India*
[7]*Division of Plant Molecular Biology and Biotechnology, Department of Biosciences, Rajagiri College of Social Sciences, Cochin, 683 104, Kerala, India*

Abstract:

Aim: To synthesize silver nanoparticles (AgNPs) using *Terminalia arjuna* bark extract (TABE) and investigate their efficacy in controlling *Aedes aegypti* and *Aedes albopictus* mosquitoes

Background: This research investigates the utilization of *Terminalia arjuna* bark extract to produce silver nanoparticles (AgNPs) as a means of controlling disease-carrying mosquitoes *Aedes aegypti* and *Aedes albopictus*. The nanoparticles are analyzed using UV-Vis spectrophotometry, XRD, FT-IR analysis, and SEM. *In silico* studies provide additional investigation into the larvicidal properties of *T. arjuna* phytochemicals, providing valuable insights into their effectiveness as biocontrol agents.

Objectives: The current research aimed to synthesize silver nanoparticles (AgNPs) using the *Terminalia arjuna* bark extract (TABE-AgNPs) in controlling the disease-transmitting vectors such as *Aedes aegypti* and *Aedes albopictus*.

Methods: The size of the synthesized nanoparticles was determined using the UV-Vis spectrophotometer, XRD, and FT-IR analysis, and the morphology of the particles was measured using the SEM. The size of the synthesized particles ranged from 28.57 to 79.38 nm. An *in silico* larvicidal and insecticidal potential of *Terminalia arjuna* chemical constituents are also carried on the key proteins of mosquitoes using the Schrodinger module.

Results: The biosynthesized AgNPs were investigated for larvicidal effect on the dengue-causing vectors such as *Aedes aegypti* and *Aedes albopictus*. The AgNPs showed a significant larvicidal impact on the mosquitoes after 24 and 48 hours, with the LC_{50} of 6.49 and 4.50 ppm, respectively. The *in-silico* research indicates that the chosen phytochemicals of *T. arjuna* exhibit larvicidal properties due to their high binding affinities with key mosquito proteins of *A. aegypti* and *A. albopictus*. Specifically, leucodelphinidin, mannitol, and leucocianidol were found to exhibit mosquitocidal properties. These revealed their insecticidal effects by showing the binding affinities and docking scores of -7.11584 kcal/mol for FK506-binding protein 12, -7.78699 kcal/mol for Arylalkylamine N-acetyltransferase 7, -5.96534 kcal/mol for salivary protein 34k2, -5.78943 kcal/mol for Odorant-binding protein and -7.21602 kcal/mol for young juvenile hormone-binding protein.

Conclusions: Eventually, the present research concluded that the phytochemicals *T. arjuna* might act as capping and reducing elements during the fabrication of nanoparticles that lead to the potential larvicidal effects after capping with silver. This study also suggested that green synthesized nanoparticles could be potential biocontrol agents in controlling the populations of disease-transmitting vectors.

Keywords: Biosynthesis, *In silico study*, Mosquitocidal, Phytochemicals, *Terminalia arjuna*, Mosquitoes.

*Address correspondence to these authors at the Department of Biosciences, Rajagiri College of Social Sciences, Cochin, 683 104, Kerala, India and Rajagiri College of Social Sciences, Cochin, 683 104, Kerala, India;
E-mails: prabhusbotany@gmail.com and antony_sm2003@yahoo.co.in

Cite as: Padmavathy B, Ebinezer B, Karthikeyan K, Arumugam M, Ayyanar M, Priya S, Amalraj S, Prabhu S, Ceasar S. *Terminalia Arjuna* (Roxb.) Wight & amp; Arn: Unveiling its Potential as a Mosquito Control Agent through Biosynthesized Nanomaterials and Computational Analysis against *Aedes Aegypti* and *Aedes Albopictus*. Open Biotechnol J, 2024; 18: e18740707325368. http://dx.doi.org/10.2174/0118740707325368240722062451

Received: May 27, 2024
Revised: July 06, 2024
Accepted: July 08, 2024
Published: July 26, 2024

1. INTRODUCTION

More than 17% of all infectious diseases are caused by vector-borne infections, which cause more than 700000 deaths annually [1]. Mosquitoes are the main vector for the spread of viruses and parasite-related diseases [1]. In particular, a wide range of viral diseases, including yellow fever, dengue, malaria, and chikungunya, are often caused by mosquitoes. *Aedes aegypti* and *Aedes albopictus* are two mosquito species that carry arboviruses and togaviruses, both of which contribute to the global health burden by transmitting a variety of viruses [2]. In general, *A. aegypti* carries flaviviruses that cause chikungunya, dengue, yellow fever, and Zika virus, whereas *A. albopictus* carries togavirus and flaviviruses that cause Ross River virus, eastern quinine virus, chickunkunya, dengue, yellow fever, and Zika virus [3].

Dengue fever is the most common viral disease and affects people worldwide [4]. There are presently 100-400 million cases reported each year, providing a health risk to almost half of the worldwide population. The number of cases registered globally increased tremendously between 2000 and 2019, from 500,000 to 5.2 million [4]. Dengue fever is transmitted primarily by the mosquito *Aedes* [2]. Since the process of developing a novel drug to treat viral infections is more difficult in terms of cost, time, and labor, vector control would be a better way to stop the transmission of such vector-borne diseases. Specifically, the ecotoxicity and chemical contaminants in soil can be considerably reduced if vector control is performed organically through novel scientific ways. Therefore, the present research aimed to develop a vector-controlling agent from plants using nanomaterials.

Nanotechnology is an emerging area of science used to improve the optical, electrical, magnetic, and catalytic properties of metal and non-metal materials for a wide range of applications, including medicine, food, cosmetics, electronics, and aerospace [5]. This field plays a key role in generating therapeutically vibrant discoveries in the biological, medical, environmental, and engineering sciences. Silver, copper, gold, titanium, platinum, zinc, magnesium, iron, and alginate nanoparticles are well-known metal-based nanomaterials [6], and titanium dioxide, silver oxide, and zinc oxide are promising metal oxide nanoparticles. Furthermore, due to the exceptional properties of nanomaterials in various biological applications, there is a growing interest among researchers in the medical field to integrate nanoparticles into a variety of disease diagnostic tools [7].

In addition to biomedical applications, nanoparticles also act as larvicidal and insecticidal agents to reduce the population of disease-causing vectors [8]. There is a need for the discovery of novel and potent larvicidal agents from medicinally important taxa that appear to be important for controlling viral transmission (Fig. **1**). Hence, green synthesis is now attracting researchers to develop novel larvicidal alternatives to disease-causing vectors. Previously, AgNPs synthesized using the *Annona glabra* leaf extract were proven to be a potential larvicidal agent against the flavivirus and tagavirus vectors, specifically *A. aegypti* and *A. albopictuss* [3]. In view of these facts, the present research has been aimed at developing a larvicidal agent from the bark of the therapeutically versatile taxon *Terminalia arjuna* (Roxb.) Wight & Arn. which belongs to the family Combretaceae, and is commonly known as Arjuna. *Terminalia arjuna* stem bark is widely used in treating a variety of ailments and is reported to have antioxidant, hypocholesterolemic, antidiabetic, anticancer, antimicrobial, antiviral, hepato-protective, anti-allergic, wound healing properties, and it is also used as natural colorant and food preservatives in food industries [9].

The present study proposed to develop a novel and potent mosquitocidal agent against disease-transmitting vectors such as *Aedes aegypti* and *Aedes albopictus*. Through this process, AgNPs were synthesized using the aqueous bark extract of *T. arjuna* as one of the reducing and stabilizing agents (TABE-AgNPs). The TABE-AgNPs were characterized with the UV-visible spectroscopy, Fourier transform infrared spectroscopy (FT-IR), X-ray diffraction analysis (XRD), Energy-dispersive X-ray spectroscopy (EDX), and scanning electron microscopy (SEM). The mosquitocidal efficacy of the biosynthesized AgNPs was tested against the *Aedes aegypti* and *Aedes albopictus* by studying their mortality by growth inhibition assessments. The study also projected into molecular docking analysis by applying the chosen bioactive compounds of *T. arjuna* with the FK506-binding protein (FKBP) from *Aedes aegypti* (2LPV), arylalkylamine N-acetyltransferases from *Aedes aegypti* (4FD7), odorant-binding protein (5V13), labrum-interacting protein, LIPS 2 (34K-2) from *Aedes albopictus* (7TDR) and odorant binding protein 1 from *Aedes albopictus*.

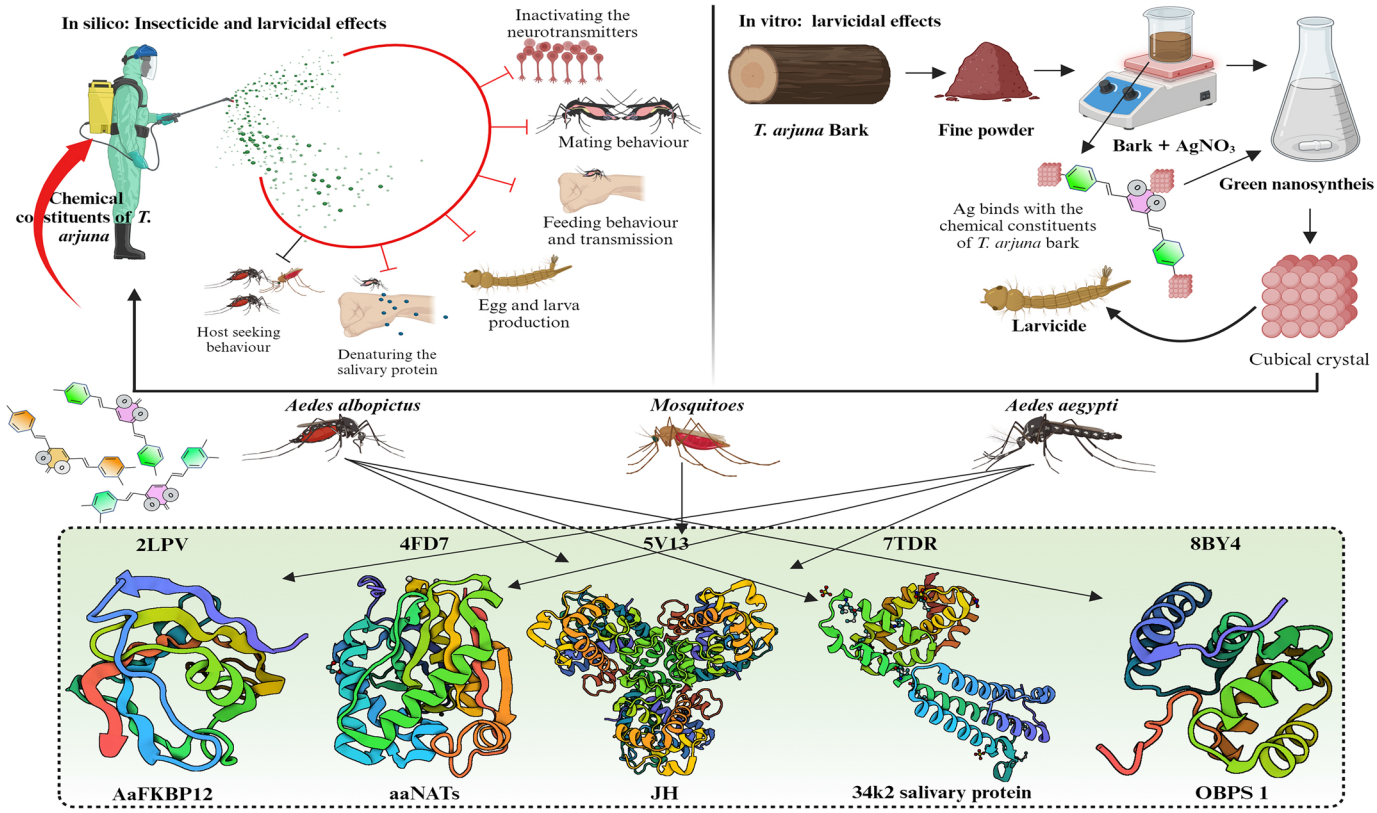

Fig. (1). Schematic representation of the research for the insecticidal and larvicidal effects of *Terminalia arjuna*.

2. MATERIALS AND METHODS

2.1. Sample Collection and Preparation of Plant Extracts

The stem bark of *T. arjuna* was collected near Kumbakonam town, Tamil Nadu, India. The plant was authenticated by a taxonomist after preparing an herbarium specimen. The harvested plant material was dried in the shade until it became crispy after being washed with tap water. The shade-dried stem bark was powdered with the electrical blender to obtain the fine powder and stored in an airtight container. The obtained powder was used further for the synthesis of silver nanoparticles. A stock was prepared by dissolving 0.1 mM of silver nitrate in 100 mL of distilled water for a stable concentration of silver ions and to avoid the decomposition of silver nitrate during the subsequent process. Since Ag is a metal-based material, anethole was employed as a capping and reducing agent of metal ions. This mixture was poured into a 250 ml conical flask and then boiled for an hour on a hot plate with a magnetic stirrer. Following the process, the mixture was cooled to collect the sedimented yield through Whatman filter paper No. 1, and the collected product was stored at 4°C for further use.

2.2. Biosynthesis of Silver Nanoparticles

Five ml of the preserved plant material was placed in a beaker containing 45 mL of AgNo3 solution. The mixture was agitated at 25±2°C for 1 hour. Later, it progressively changes color from reddish brown to yellow. It was observed as a visual representation of silver manufacture. The reaction solution was then centrifuged at 8000 rpm for 40 mins, and the sedimentation was collected for further centrifugation at 14000 rpm. Eventually, the collected material was dehydrated with ethanol, dried with a desiccant, and kept to assess its larvicidal properties.

2.3. Optical and Spectral Characterization

The biosynthesized silver nanoparticles (TABE-AgNPs) were characterized by a variety of optical methods, including UV-Vis spectroscopy, FTIR, scanning electron microscopy (SEM), and energy-dispersive X-ray (EDX) spectroscopy. Initially, to determine the presence of silver in the extract, the absorption spectra of silver nanoparticles were examined at 300 and 540 nm with a UV–vis spectrophotometer (Hitachi U-2001). The spectrum was taken at various intervals up to 24 hours after the addition of $AgNO_3$ to the extract, as shown in the nanoparticle synthesis process. Additionally, to determine the functional groups, the green synthesized nanoparticles were subjected to FT-IR analysis (Perkin Elmer model spectrum RX 1), where the synthesized material was examined in the spectral range of 400 cm^{-1} to 4000 cm^{-1}. Prior to the FT-IR analysis, the sample was dried at 75°C. The phase composition and size of the synthesized

material were then assessed using XRD (Malvern Panalytical, Malvern Instrument Limited, UK) and EDX (Model-D8 Advance, Bruker, Germany). The morphological structure of the engineered nanomaterials was measured by SEM.

2.4. *In Vitro* Larvicidal Activity

2.4.1. Culture Maintenance

The larvae of *Aedes aegypti* and *Aedes albopictus* were reared in the vector control center at Government Arts College, Kumbakonam, India. During the process, the cultures were maintained at a temperature of 28±2°C and humidity of 75±5% with a photoperiod of 12±5 hrs. Subsequently, the larvae of *A. aegypti* and *A. albopictus* were placed in a plastic container with 500 mL of water, where they were kept to avoid contamination, repellency, and insecticidal effects [10]. Finally, the F1 generation of the raised larvae was used to assess the larvicidal effects of the TABE-AgNPs.

2.4.2. Larvicidal Effects

The larvicidal effect of the TABE-AgNPs was explored according to the guidelines of the [11]. Briefly, five batches of third-instar larvae of uniform size, hale, and healthy individuals were used in this experiment; they ranged in age from 0 to 6. Then, they were transferred into a transparent beaker containing 100 mL of water (in a 250 mL beaker). Then, the larvae were treated with TABE-AgNPs at a concentration of 10, 20, 40, 60, 80, and 100 µg/mL in a dose-dependent manner. Five replications were maintained for each concentration. For the toxicity assay, a wide and narrow concentration range was tested, and the mortality rate of the larvae was determined every 12 hrs for 24 hrs in the following method [12].

$$\text{a).Mortality} = \frac{\text{Number of dead larvae}}{\text{Number of larvae introduced}}$$

$$\text{b). Corrected Percentage of Mortality} = \frac{1-\text{n T after treatment}}{1-\text{n C after treatment}}$$

n denotes the number of larvae, T denotes the number of treated larvae, and C denotes the number of control larvae. The tailored percentage mortality value for each concentration was examined to determine its LC_{50} values by utilizing US EPA probit analysis software (V 1.5).

2.5. Statistical Analysis

Five replications were performed for each concentration. In addition, to determine the lethal concentrations of treatment (LC_{50} and LC_{90}), the observed larval mortalities were adjusted using Abbott's formula. The larval mortality rates for each concentration are given as the mean ± standard deviation [13]. The larvicidal analysis was carried out through a one-way analysis of variance (ANOVA). The significant levels between treatment groups were explored using a Tukey's multiple test ($p \leq 0.05$).

2.6. *In Silico* Studies for the Larvicidal, Insecticidal and Repellent Activities

2.6.1. Biological Sources

A total of 41 chemical constituents of *Terminalia arjuna* were obtained from the Indian medicinal plant database (IMPAAT 2.0), which contains nearly 18000 chemical constituents from 4010 Indian medicinal plants [14]. Targets such as FK506-binding protein (FKBP) from *Aedes aegypti* (2LPV), arylalkylamine N-acetyltransferases from *Aedes aegypti* (4FD7), odorant-binding protein family member specifically binds juvenile hormone (5V13), Labrum-interacting protein from saliva LIPS 2 (34K-2) from *Aedes albopictus* (7TDR) and odorant binding protein 1 from *Aedes albopictus* were retrieved from the Protein Databank (https://www.rcsb.org/) for exploring the larvicidal and insecticidal potential of *Aedes aegypti* and *Aedes albopictus*.

2.6.2. Ligand and Protein Preparation

The retrieved ligands and proteins for the present *in silico* research were prepared by Maestro V. 13.8. Additionally, to reduce physical complexity, the ligands were prepared using the LigPrep tool. Similarly, the proteins were initially examined with a protein preparation tool to remove HETs and water molecules. This tool also assisted in updating any residues that were missing from the side chain and backbone. Subsequently, all the targets were subjected to a SiteMap assessment to determine the potential receptor sites for ligand binding. Moreover, using the glidegride module, an active site in each receptor was fixed as a stable site for ligand binding [15].

2.6.3. Molecular Docking

In addition, to perform the molecular docking, each glide-constructed target was first loaded into the glide-based ligand docking modules. The prepared ligands were then loaded into this module. To soften the potential for nonpolar ligand parts, the vdW radii of ligand atoms with partial atomic charges were set to 0.80 and 0.15. Similarly, to determine the exact docking scores and binding affinities of the chemical constituents of *T. arjuna* against *A. aegypti* and *A. albopictus*, the Xtra precision module was used for rigid ligand sampling [16].

3. RESULTS AND DISCUSSION

3.1. Optical Characterization

3.1.1. UV–Vis Spectroscopy

The plant extract enhanced the reduction of silver ions, resulting in silver nanoparticles, as evidenced by the observed color changes. AgNPS production requires surface plasmon resonance (SPR) vibration, which is only triggered by Ag+ ion reduction. Similarly, when a green-based silver nanosynthesis was developed in *T. arjuna* bark-mediated extract, the polyphenols and proteins of *T. arjuna* significantly reduced the amount of Ag+ ions [17]. This shows that the bark of *T. arjuna* has a broad and strong surface plasmon resonance for green-mediated nanosynthesis. Consistent with this statement, a powerful indication related to silver nanoparticles was found at approximately 440 nm (Fig. **2a**). The absorption intensity

of metal ions is quick, with a decrease of more than 90% in Ag+ ions obtained in 4 hours. Finally, the UV–Vis spectrum demonstrated that the metal ion concentration in the bark of *T. arjuna* decreased upon the addition of silver.

3.1.2. FTIR Analysis

The functional groups (carboxyl, hydroxyl, and carbonyl) of phytochemicals that encapsulate and successfully sustain nanoparticles with plant extracts were found using the FT-IR. The IR spectra revealed significant peaks at 3480.20 (OH-stretching), 2980.40 (CH-stretching), 2950.30 (CH-stretching), 1700.30 (CO-stretching), 1050.10 (CO-stretching), 950.20 (COC-stretching), 800.30 (aromatic compound) and 1500.20 (phenol ring). The synthesized silver nanoparticles showed a peak between 3490 and 3500 cm^{-1}, which corresponds to the stretching of O-H bonds in hydrogen-bonded alcohols and phenols. Furthermore, the peak at 1500-1550 cm^{-1} was attributed to the stretching of the C-H bond, while the peak at 1450-1500 cm^{-1} was attributed to the stretching of the N-H bond (Fig. **2b**). Based on these FTIR investi- gations, we noticed that carbonyl groups in amino acid residues and proteins were very susceptible to metal binding. This shows that the protein may have a function in preventing metal nanoparticle aggregation and managing the environment surrounding it [18]. The polyphenols, phenolic acids, and proteins of the stem bark extract also contributed to the decrease in silver ions, which agrees with the previously published reports [17, 19]. These concerns can be addressed by isolating, identifying, and testing the chemical ingredients of plant extracts to determine the effectiveness of plants in reducing metal ions.

3.1.3. XRD Analysis

The XRD is used to determine the crystalline structure and grid characteristics of the TABE-AgNPs production, where the 2θ of the synthesized material ranged from 10-60°, as shown in Fig. (**2c**). The XRD pattern indicated that the synthesized material (AgNPs) had seven strong peaks located at 18°, 22°, 27°, 34°, 36°, 42°, and 50°. There was a peak with a maximum intensity of 27°, which corresponded to an identical structural orientation. A few more peaks appeared in the plot, which might be attributed to the existence of the biological components of the extract. According to Mollic *et al*. [20], smaller particle sizes are shown by larger peaks, which also indicate how experimental circumstances influence the nucleation and crystal nucleation processes.

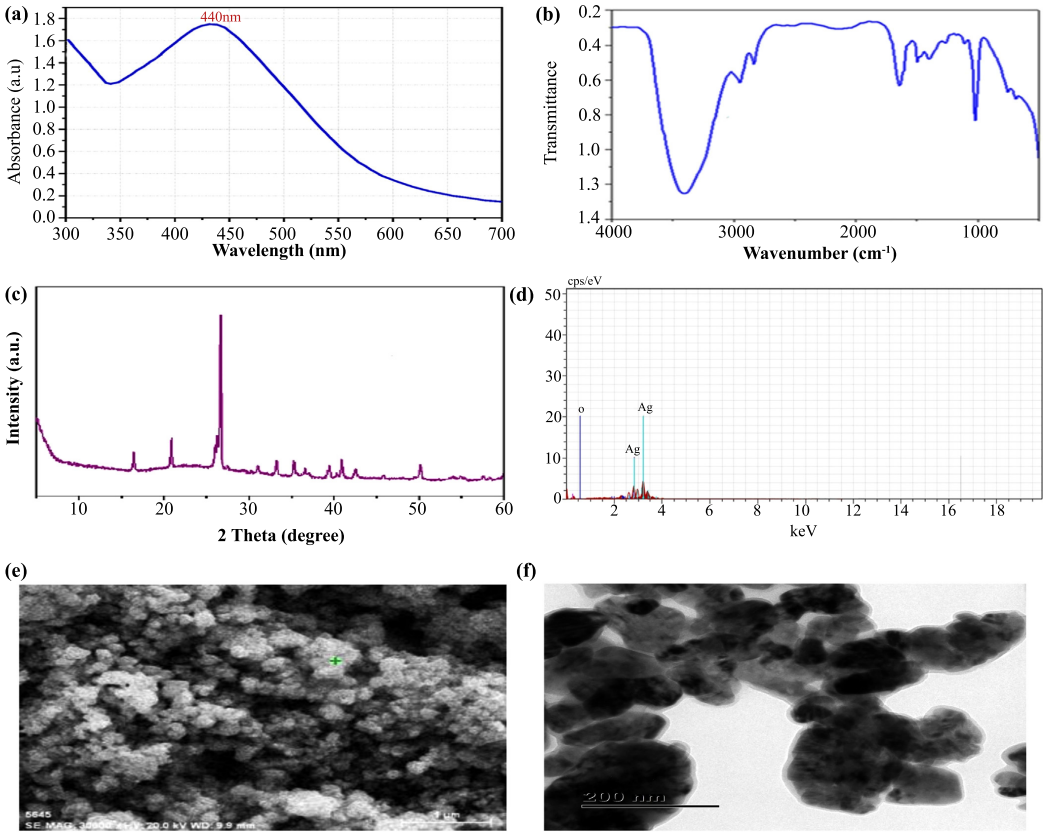

Fig. (2). Optical characterization of green synthesised AgNPs: (**a**). UV- Vis Spectrum shows the wavelength of Silver, (**b**). FT-IR shows the functional groups of plant chemical constituents that bind with the silver, (**c**). The spectrum of XRD, (**d**). Spectrum of Energy-dispersive X-ray spectroscopy (EDX) and (**e-f**). SEM and TEM images show the morphology of particle

3.1.4. EDX and SEM

The EDX analysis confirmed that the silver ions had two distinct peaks with weight percentages of 22% and 10% (Fig. **2d**). Furthermore, the peak for oxygen at 20% was found to be equivalent to that of silver (Ag). The signal for oxygen (O) indicated that the surface of the prepared material (TABE-AgNPs) had potentially absorbed extracellular organic material [13]. In a recent study, a weak signal of Al along with strong silver pear was observed in the biosynthesized silver nanoparticles using *T. arjuna* bark extract. Since the detection limit of silver is higher than that of all the other trace elements in the sample, they claimed that the existence of a strong silver peak and a faint signal of Al may be the presence of biomolecules adhering to the surface of the synthesized material [17]. Using SEM, the morphology and shape of the synthesized silver nanoparticles were measured. Based on the SEM image, it was found that the synthesized AgNPs had a crystalline structure and cubical shape with a size ranging from 45 to 60 nm (Fig. **2e**). The particles have an average size of 52 nm [21].

3.2. *In Vitro* Larvicidal Effects of T. arjuna Bark AgNPs

3.2.1. Larvicidal Impact of T. arjuna Bark AgNPs on Aedes Albopictus

The larvicidal effect of the TABE-AgNPs was investigated on the larvae of *A. aegypti* and *A. albopictus* at various concentrations revealing that the generated nanoparticles were considerably harmful to the 3rd instar larvae of *A. aegypti* at all treatment dosages. The mobility (leading to mortality) of *A. albopictus* larvae notably decreased after 12 hours of exposure with reductions of 20% at 10 µg/mL, 33% at 20 µg/mL, 46% at 40 µg/mL, 61% at 60 µg/mL, 81% at 80 µg/mL, and 86% at 100 µg/mL (Table **1**). The LC_{50} of the TABE-AgNPs against the *A. albopictus* larvae was recorded as 82 µg/mL. After 24 hrs of exposure, the effect of TABE-AgNPs on the mortality rate of larvae was also investigated. The extracts reduced the larval mobility (leads to mortality) by 22% at 10 µg/mL, 42% at 20% µg/mL, 52% at 40 µg/mL, 82% at 60 µg/mL, 86% at 80 µg/mL, and 88% at 100 µg/mL (Table **1**). Compared with the 12-hour treatment, a slightly lower LC_{50} dose was required to inhibit the growth of *A. albopictus* larvae.

Previous researches demonstrated that the silver nanoparticles synthesized *via* the green route had significant ovicidal and larvicidal effects on disease-causing vectors like, *Aedes aegypti*, *Anopheles stephensi*, *Anopheles subpictus*, *Aedes albopictus*, and *Culex quinquefasciatus* [3, 22, 23]. The dose-dependent larvicidal and ovicidal effects of *Carissa carandas*-mediated silver nanoparticles against the vectors *Anopheles stephensi*, *Aedes aegypti*, and *Culex quinquefasciatus* were reported by [24] with significant insecticidal effects on all the treated vectors with the LC_{50} of 14.33, 15.69, and 16.95 µg/mL, respectively. Similarly, the larvicidal effects of *Barleria cristata*-synthesized AgNps had significant insecticidal effects with the LC_{50} of 12.46, 13.59, and 15.01 µg/mL against the third-instar larvae of *Anopheles subpictus*, *Aedes albopictus*, and *Culex tritaeniorhynchus* mosquitoes, respectively [25]. The AgNPs synthesized using *Mimusops elengi* also showed significant larvicidal and pupicidal effects on *A. stephensi* and *A. albopictus* after treatment at low doses [26]. Since green-synthesized nanoparticles are tiny enough to penetrate through insect cuticles and enter individual cells, where they obstruct molting and other physiological processes, it is possible that this is the cause of the harmful effects of AgNPs on mosquitoes [27].

3.2.2. Larvicidal Impact of T. arjuna Bark AgNPs on Aedes Aegypti

Similar to the larvicidal evaluation of *A. albopictus*, the larvicidal effects of TABE-AgNPs on the larvae of *A. aegypti* were also investigated. The results revealed that TABE-AgNPs were harmful to 3rd instar larvae of *A. aegypti* at all treatment dosages. After 12 hours, the larval migration rates decreased significantly with 14% at 10 µg/mL, 26% at 20 µg/mL, 39% at 40 µg/mL, 51% at 60 µg/mL, 76% at 80 µg/mL, and 84% at 100 µg/mL (Table **1**). The LC_{50} of the TABE-AgNPs for *A. aegypti* larvae was determined to be 101.1 µg/mL. After 24 hrs of exposure, the effect of TABE-AgNPs on the mortality rate of larvae was also studied, and the extracts reduced larval mobility (leads to mortality) by 22% at 10 µg/mL, 34% at 20 µg/mL, 44% at 40 µg/mL, 58% at 60 µg/mL, 63% at 80 µg/mL and 70% at 100 µg/mL. The larvicidal effects of *T. arjuna* bark extracts on *Aedes aegypti* were previously studied at various concentrations (10, 25, 50, 100 and 200 µg/mL) after the extracts were prepared with hexane, chloroform, ethyl acetate, and methanol [24]. In the extracts the chloroform extract showed a high mortality rate at all doses, with the LC_{50} and LC_{90} of 4.61 and 24.12 µg/mL, respectively. *Carissa carandas*-powered silver nanoparticles on the vectors *Anopheles stephensi, Aedes aegypti,* and *Culex quinquefasciatus* exhibited substantial ovicidal and larvicidal effects than crude plant extract treatment [24]. It was reported that the ability of nanoparticles to penetrate mosquito exoskeletons causes biotoxicity in mosquitos, particularly juvenile instars [28]. The nanoparticles can bind sulfur from proteins or phosphorus of DNA, triggering rapid denaturation of organelles and enzymes in the intracellular space of mosquito larvae and pupae, which ultimately leads to death. Subsequently, cellular malfunction and cell death are triggered in mosquitoes by decreased membrane permeability and disruption of proton motive force [3, 29].

3.3. *In Silico* Larvicidal and Insecticidal Effects

In general, toxic chemicals found in plant extracts are secondary metabolites that develop defense systems from foreign pathogens, mainly herbivores [30]. These chemical compounds may attack the insect body in several ways through various methods of action. Insects that consume these secondary metabolites may come into contact with hazardous materials that may impact a variety of

molecular targets, such as receptors, enzymes, signaling molecules, ion channels, and structural proteins, namely, nucleic acids, biomembranes, and other cellular components [31]. Furthermore, to screen the unique mode of action of *T. arjuna* phytochemicals as insecticidal agents, the present study selected five essential mosquito targets that are primarily responsible for mosquito populations, growth, and survival.

Table 1. Larvicidal activity of synthesized silver nanoparticles using *Terminalia arjuna* bark extract against *Aedes albopictus* and *Aedes aegypti* reared larvae.

Name of the Mosquito species	Exposure Period (hour)	Conc. (µg/ml)	% Mortality ± Standard Error	LC_{50} (LCL-UCL) [a]	LC_{90} (LCL-UCL) [a]	X^2(d=4) [b]
Aedes albopictus	12	Control	0±0	82.1 (73.2-121.5)	143.1 (142.1-162.1)	6.13
		10	20.3± 0.23			
		20	33.1±0.27			
		40	46.1±0.35			
		60	61.3±0.14			
		80	81.5±0.15			
		100	86.12±0.54			
	24	Control	0±0	71.3 (61.2-94.1)	134.2 (132.0-148.2)	1.22
		10	22.0±0.28			
		20	42.1±0.56			
		40	52.1±0.16			
		60	82.3±0.31			
		80	86.1±0.27			
		100	88.2±0.21			
Aedes aegypti	12	Control	0±0	101.1 (64.1-90.3)	143.4 (92.1-121.4)	4.27
		10	14.1±0.18			
		20	26.1±0.37			
		40	39.1±0.43			
		60	51.4±0.19			
		80	76.1±0.21			
		100	84±0.34			
	24	Control	0±0	75.1 (66.5-86.4)	127.3 (78.1-136.7)	4.1
		10	22.3±0.24			
		20	34.0±0.25			
		40	44.0±0.18			
		60	58.0±0.11			
		80	63.0±0.27			
		100	70.1±0.2			

Note: Control-nil activity, SE-standard error, LCL-lower confidence level, UCL-upper confidence level [a]95% confidence interval, b Degree of freedom, X^2-Chi-Square value.

Table 2. Docking scores, Van Der Waals Forces, and glide energies of *T. arjuna* chemical constituents against FK506-binding protein 12 of *Aedes aegypti* (2LPV).

S.No.	Name of the Chemical Constituents	Phytochemical ID No. in IMPPAT 2.0	Docking Scores (Kcal/mol)	ΔGvdW	Glide Energy
1.	Leucodelphidin	IMPHY011885	-7.11584	-23.8298	-27.5446
2.	Leucocianidol	IMPHY011611	-5.9172	-23.7584	-25.8646
3.	(+)-Leucocyanidin	IMPHY011966	-5.8045	-23.5226	-25.6802
4.	Mannitol	IMPHY011729	-5.76079	-11.7054	-18.9409
5.	(+)-Gallocatechin	IMPHY011735	-5.56912	-16.2104	-24.2848
6.	Baicalein	IMPHY005607	-5.5416	-21.7174	-22.062
7.	Arjunolone	IMPHY002418	-5.43098	-23.5223	-25.6366
8.	Epigallocatechin	IMPHY011737	-4.46131	-20.7234	-20.3217
9.	Ellagic acid	IMPHY005537	-4.18609	-19.0283	-25.0839
10.	Catechol	IMPHY004079	-3.91459	-9.09966	-15.8819
11.	Gallic acid	IMPHY012021	-3.88247	-11.9317	-17.9788

(Table 2) contd.....

S.No.	Name of the Chemical Constituents	Phytochemical ID No. in IMPPAT 2.0	Docking Scores (Kcal/mol)	ΔGvdW	Glide Energy
12.	2,3-(S)-hexahydroxydiphenoyl-D-glucose	IMPHY000896	-3.64452	-19.7968	-26.7233
13.	8-Hydroxyhexadecanoic acid	IMPHY011699	-3.55891	-15.3773	-22.7753
14.	Arjunjenin	IMPHY012650	-2.78727	-16.2246	-15.172
15.	β-sitosterol	IMPHY014836	-2.4083	-15.5747	-16.2498
16.	Maslinic acid	IMPHY011970	-2.39777	-19.4719	-20.0016
17.	Afrormosin	IMPHY004562	-2.28417	-19.2269	-19.3939
18.	Methyl oleanolate	IMPHY011461	-1.9787	-21.3179	-21.2361
19.	Oxalic acid	IMPHY007450	-1.65619	-6.3013	-9.4315
20.	Terminic acid	IMPHY008675	-1.61667	-20.3637	-20.9046
21.	Friedelin	IMPHY011688	-1.32045	-17.491	-18.2001

3.3.1. FK506-binding Protein 12 from Aedes Aegypti (2LPV)

Dengue fever remains one of the most serious health issues because the virus can invade the immune system. Currently, there are no drugs or vaccines available for the prevention of dengue. However, the immunosuppressant FK506 has been used as a drug to combat the dengue virus by binding with the FKBP binding protein of human *Plasmodium* parasites. The same protein, AaFKBP12, was also found in *Aedes aegypti* [32]. Moreover, due to the binding nature of this protein, they reported that it could be a therapeutic target to inhibit the dengue transmission vector. Therefore, the present research utilized this protein for its immunosuppressive effect on the FKBP12 of *T. arjuna* phytochemicals.

Nearly 38 chemical components of *T. arjuna* were coupled with the AaFKBP12 protein to determine its inhibitory effect on pathogen transmission by *A. aegypti*. Among the docked phytochemicals, 21 were found to be active molecules for binding to FKBP12 of *A. aegypti* (Table **2**). In particular, leucodelphinidin had a docking score of -7.11584 Kcal/mol with strong hydrogen bonding interactions. Subsequently, several other chemical components, namely, leucocyananidol, (+)-leucocyanidin, mannitol, (+)-gallocatechin, baicalein, and arjunolone, were found to have moderate docking values ranging from -5.9172 Kcal/mol to -5.43098 Kcal/mol (Table **2**). The remaining molecules had the lowest docking values below -4.46131 Kcal/mol, but each had a hydrogen bond with distances less than 3.0 Å.

Leucodelphinidin has two hydrogen bond contacts with residues of the FK506-binding protein of *A. aegypti*. This molecule has demonstrated its insecticidal activity by targeting residues ASP 32 and VAL 91 (Fig. **3a**). The contact distances were 2.12 for ASP 38 and 2.41 for VAL 91, and these binding affinities were established with the hydroxyl group of leucodelphinidin (Fig. **3b** and Table **2**). Furthermore, Leucocianidol had the second-highest docking score as an insecticidal agent. Two hydrogen bonding interactions with the target residues of VAL91 and ASP32 have been established, which matches the number of binding affinities of leucodelphinidin (Fig. **3c**). The contact distances of this molecule were 2.70 for VAL 91 and 2.27 for ASP 38, and these binding affinities were established with the hydroxyl groups of Leucocianidol (Fig. **3d**).

3.3.2. Arylalkylamine N-acetyltransferase 7 from the Yellow Fever Mosquito Aedes aegypti (4FD7)

It catalyzes the transacetylation of acetyl-CoA to arylalkylamine. aaNATs play a role in insect sclerotization and neurotransmitter inactivation [33]. Since aaNATs are capable of inactivating neurotransmitters in insects, this protein was used in the present research to identify the active insecticidal ingredients from *T. arjuna*. Of the docked molecules, 21 were also found to be active candidates for stimulating arylalkylamine N-acetyl-transferase 7, showing that they may exert an insecticidal effect by inactivating mosquito neurotransmitters. In particular, chemical components such as mannitol, leucocianidol, and ellagic acid were found to be active candidates with docking values of -7.78699 Kcal/mol, -6.78264 Kcal/mol and -6.31408 Kcal/mol, respectively (Table **3**). In addition, other metabolites, namely, epigal-locatechin, arjunolone, (+)-leucocyanidin, (+)-gallocatechin, gallic acid, epigallocatechin and leucodel-phidin, were also identified as active candidates for causing insecticidal effects. These compounds had moderate docking scores ranging from -5.39032 to -5.04139 (Table **3**).

Based on the docking scores, the chemical components mannitol and leucocianidol were investigated for their binding affinity with aaNATs. Mannitol has a strong binding affinity, showing five hydrogen bond interactions with aaNAT residues. ASP 105, TYR 126, ASP 113, and ASP 111 were revealed to be essential residues for these significant binding affinities with mannitol (Fig. **4a**). It is interesting to note that ASP 105 has covalent interactions with the target. The hydrogen bond distance measurements indicated that the number of interactions between mannitol and aaNATs was 1.76 for APS 113, 2.15 and 1.64 for ASP 105, 2.16 for ASP 111, and 1.99 for TYR 126 (Fig. **4a**). All of these contacts were established with the hydroxyl groups of mannitol, as shown in Fig. (**4b**). On the other hand, the molecule known as leucocianidol had the second-highest docking score. As a result, the binding affinities of this molecule for aaNATs were also assessed, where it revealed three hydrogen bond contacts with residues ASP 113 (1.92), ASP 84 (2.17), and LYS 2 (1.85) (Fig. **4c**). All of these interactions were established with the hydroxyl groups of leucocianidol (Fig. **4d**).

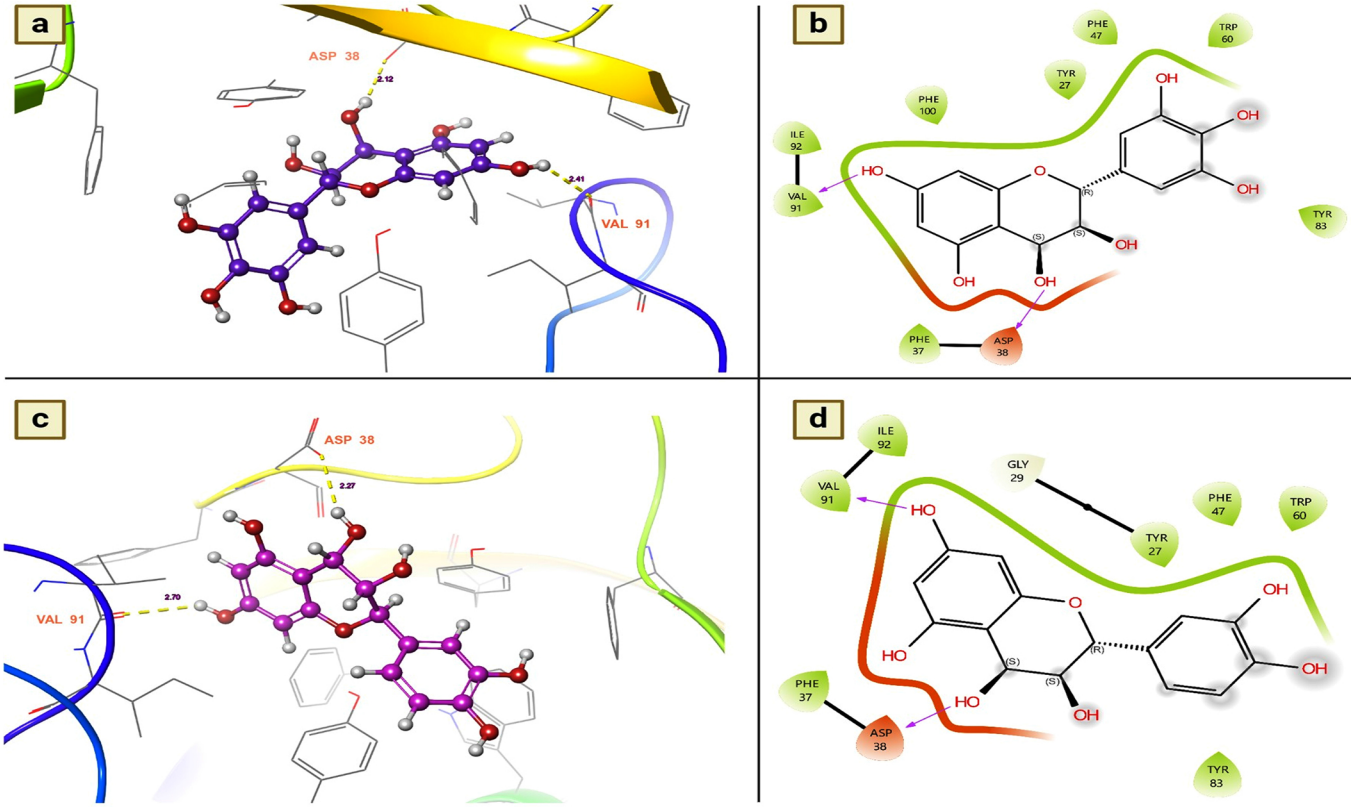

Fig. (3). (**a** and **b**). Leucodelphinidin shows the residues and hydrogen bond contacts with Aa FKB12; (**c** and **d**). Leucocianidol shows the residues and hydrogen bond contacts with Aa FKB12.

Table 3. Docking scores, Van Der Waals Forces and glide energies of *T. arjuna* chemical constituentsagainst Arylalkylamine N-acetyltransferase 7 of yellow fever mosquito *Aedes aegypti* (4FD7).

S.No	Name of the Chemical Constituents	Phytochemical ID No. in IMPPAT 2.0	Docking Scores (Kcal/mol)	ΔGvdW	Glide Energy
1.	Mannitol	IMPHY011966	-7.78699	-30.8833	-31.1198
2.	Leucocianidol	IMPHY005537	-6.78264	-27.4079	-31.8438
3.	Ellagic acid	IMPHY011729	-6.31408	-10.6145	-32.1724
4.	Epigallocatechin	IMPHY011737	-3.19233	-29.2256	-31.872
5.	Arjunolone	IMPHY002418	-5.39032	-25.1792	-26.8575
6.	(+)-Leucocyanidin	IMPHY011611	-5.2203	-21.5864	-33.2768
7.	(+)-Gallocatechin	IMPHY011735	-5.18536	-29.9992	-38.4342
8.	Gallic acid	IMPHY012021	-5.09799	-24.2508	-25.0889
9.	Epigallocatechin	IMPHY011737	-5.04705	-26.063	-32.976
10.	Leucodelphidin	IMPHY011885	-5.04139	-27.8916	-32.6957
11.	Catechol	IMPHY004079	-4.37297	-18.879	-22.6247
12.	Cerasidin	IMPHY002542	-3.92435	-43.7416	-43.1524
13.	Afrormosin	IMPHY004562	-3.52422	-29.5928	-30.8091
14.	Baicalein	IMPHY005607	-0.73547	-35.5336	-39.2604
15.	Oxalic acid	IMPHY007450	-2.66961	-6.78814	-12.919
16.	8-Hydroxyhexadecanoic acid	IMPHY011699	-2.47789	-1.96159	-0.352181
17.	Stearate	IMPHY004097	-2.46225	-13.1955	-17.411
18.	Arjunone	IMPHY008708	-2.38735	-24.2211	-24.457
19.	8-Hydroxyhexadecanoic acid	IMPHY011699	-1.5766	-16.4624	-15.9004
20.	Arjunic acid	IMPHY001431	1.99336	-17.1237	-18.5633

(Table 3) contd.....

S.No	Name of the Chemical Constituents	Phytochemical ID No. in IMPPAT 2.0	Docking Scores (Kcal/mol)	ΔGvdW	Glide Energy
21.	Terminic acid	IMPHY008675	2.51818	-13.3902	-9.26195

3.3.3. Juvenile Hormone-binding Protein of Mosquito (5V13)

Juvenile hormone (JH) is the key hormone of the mosquito and plays various roles in the physiological behavior of the mosquito, especially in the development of eggs and larvae, reproduction (higher egg production), resistance development (repellent resistance), behavioral modification (matting, feeding and oviposition) and vector competence (transmission of pathogens) [34]. Since suppressing this hormone could be a feasible target for mosquito control, the present study investigated the inhibitory effects of *T. arjuna* phytoconstituents on JH. Furthermore, to determine whether the chemical components of *T. arjuna* have a suppressive effect on mosquito JH, nearly 38 chemical components were docked to this protein. Of the docked chemical components, 32 chemical components were found to be active candidates for inhibiting disease transmission vectors, particularly mosquitoes, by showing a disrupting potential for this hormone (Table **4**). Of these, mannitol has emerged as a notable candidate for inhibiting this hormone, followed by leucocianidol (-6.61762 Kcal/mol), leucodelphidine (-6.34841 Kcal/mol), ellagic acid (-6.06327 Kcal/mol), arjunjenin (-5.94011 Kcal/mol), (+)-leucocyanidin (-5.75252 Kcal/mol), (+)-gallocatechin (-5.48612 Kcal/mol) and maslinic acid (-5.33025 Kcal/mol) (Table **4**).

The binding affinities of mannitol and Leucocianidol were investigated to provide insight into their suppressive effects and the residues they selectively target to induce these hormone-suppressive effects. The present study revealed that mannitol established five hydrogen bond interactions, which resulted in robust bonds with the target. The key residues responsible for the substantial binding affinity between the target and mannitol were GLU 205, GLN 28, GLY 71, ARG 201, and ARG 198. These interactions were measured at 1.74 for GLU 205, 2.23 for GLN 28, 1.72 for GLN 71, 2.26 for ARG 201, and 2.31 for ARG 198 (Fig. **5a**). All of these interactions were established with the hydroxyl groups of mannitol (Fig. **5b**). On the other hand, the molecule known as leucocianidol had the second-highest docking score against this protein. The binding affinities of this molecule for the mosquito juvenile hormone-binding protein were also assessed, where it showed nearly three hydrogen bond contacts with residues ARG 201 (2.27), GLU 27 (2.15), and GLU 161 (1.98) (Fig. **5c**). All of these interactions were established with the hydroxyl groups of leucocianidol (Fig. **5d**).

Table 4. Docking scores, Van Der Waals Forces and glide energies of *T. arjuna* chemical constituents against Juvenile hormone-binding protein of Mosquito (5V13).

S.No.	Name of the Chemical Constituents	Phytochemical ID No. in IMPPAT 2.0	Docking Scores (Kcal/mol)	ΔGvdW	Glide Energy
1.	Mannitol	IMPHY011885	-7.21602	-21.9814	-36.8239
2.	Leucocianidol	IMPHY011729	-6.61762	-10.6116	-27.4103
3.	Leucodelphidin	IMPHY011611	-6.34841	-29.0942	-32.5928
4.	Ellagic acid	IMPHY005537	-6.06327	-26.4479	-33.7432
5.	Arjunjenin	IMPHY012650	-5.94011	-20.2422	-32.8488
6.	(+)-Leucocyanidin	IMPHY011966	-5.75252	-31.5928	-30.9328
7.	(+)-Gallocatechin	IMPHY011735	-5.48612	-30.9637	-31.049
8.	Maslinic acid	IMPHY011970	-5.33025	-26.0905	-29.4049
9.	Epigallocatechin	IMPHY011737	-4.90232	-29.8998	-37.7646
10.	2,3-(S)-hexahydroxydiphenoyl-D-glucose	IMPHY000896	-4.81169	-34.2027	-37.9881
11.	Arjunone	IMPHY008708	-4.71933	-24.2399	-26.8616
12.	Oleanolic acid	IMPHY011826	-4.70822	-28.5376	-33.0443
13.	Afrormosin	IMPHY004562	-4.60947	-27.4267	-30.7955
14.	Arjunglucoside I	IMPHY013222	-4.5952	-19.9781	-35.0436
15.	Gallic acid	IMPHY012021	-4.29414	-18.2989	-21.3956
16.	Arjunolone	IMPHY002418	-4.14452	-24.5521	-30.4838
17.	Catechol	IMPHY004079	-3.88357	-15.9119	-20.8877
18.	[(2S,3R,4S,5S,6R)-6-hydroxy-3,4,5-tris[(3,4,5-trihydroxybenzoyl) oxy] tetrahydropyran-2-yl] methyl 3,4,5-trihydroxybenzoate	IMPHY010360	-3.78387	-32.8759	-35.9229
19.	Tomentosic acid	IMPHY012649	-3.58269	-20.7907	-32.2507
20.	2α,3β,23-trihydroxyolean-12-en-28-oic acid 28-O-β-D-glucopynoside	IMPHY008919	-3.49086	-21.0762	-24.001
21.	Stearate	IMPHY004097	-3.40492	-20.4179	-20.9723
22.	Epigallocatechin	IMPHY011737	-3.35314	-27.8069	-26.117
23.	Cerasidin	IMPHY002542	-3.18588	-27.619	-30.8338
24.	Oxalic acid	IMPHY007450	-2.81656	-7.04943	-5.30205

(Table 4) contd.....

S.No.	Name of the Chemical Constituents	Phytochemical ID No. in IMPPAT 2.0	Docking Scores (Kcal/mol)	ΔGvdW	Glide Energy
25.	8-Hydroxyhexadecanoic acid	IMPHY011699	-2.81271	-18.1411	-21.9245
26.	β-sitosterol	IMPHY014836	-2.54706	-24.4877	-27.7842
27.	Arachidic acid	IMPHY011394	-2.41399	-21.9184	-23.8714
28.	Hentriacontane	IMPHY008910	-1.91983	-24.4347	-24.4524
29.	Friedelin	IMPHY011688	-1.84724	-29.7184	-28.1538
30.	Methyl oleanolate	IMPHY011461	-1.69385	-28.7491	-30.7651
31.	Myristyl oleate	IMPHY005947	-1.2626	-20.1861	-22.5673
32.	Baicalein	IMPHY005607	-0.898939	-27.692	-24.1283

Table 5. Docking scores, Van Der Waals Forces and glide energies of *T. arjuna* chemical constituents against Salivary protein 34k2 of *Aedes albopictus* (7TDR).

S.No.	Name of the Chemical Constituents	Phytochemical ID No. in IMPPAT 2.0	Docking Scores (Kcal/mol)	ΔGvdW	Glide Energy
1.	Leucocianidol	IMPHY011611	-5.96534	-11.6218	-32.1413
2.	Leucodelphidin	IMPHY011885	-5.87135	-22.4237	-37.8853
3.	2,3-(S)-hexahydroxydiphenoyl-D-glucose	IMPHY000896	-5.74165	-24.9407	-35.1688
4.	Gallic acid	IMPHY012021	-4.70356	-9.92681	-21.2616
5.	Mannitol	IMPHY011729	-4.52336	-15.9934	-21.1846
6.	Ellagic acid	IMPHY005537	-4.42596	-23.4102	-27.3423
7.	8-Hydroxyhexadecanoic acid	IMPHY011699	-3.69135	-16.7395	-22.8599
8.	Arjunetin	IMPHY005514	-3.64395	-20.0011	-22.7676
9.	(+)-Gallocatechin	IMPHY011735	-3.47957	-19.8393	-24.5
10.	(+)-Leucocyanidin	IMPHY011966	-3.14869	-16.8885	-29.0468
11.	Arjunglucoside I	IMPHY013222	-2.99009	-21.8911	-25.2476
12.	Epigallocatechin	IMPHY011737	-2.94301	-19.3533	-23.821
13.	Tomentosic acid	IMPHY012649	-2.82649	-18.0226	-26.1203
14.	Catechol	IMPHY004079	-2.53188	-8.07312	-15.9451
15.	Oleanolic acid	IMPHY011826	-2.34161	-26.7748	-31.3301
16.	Cerasidin	IMPHY002542	-2.2496	-17.7764	-25.5294
17.	Maslinic acid	IMPHY011970	-2.14886	-20.9449	-26.5821
18.	Oxalic acid	IMPHY007450	-2.13352	-2.21684	-9.20006
19.	Arjunjenin	IMPHY012650	-2.08424	-17.6211	-22.0885
20.	Stearate	IMPHY004097	-2.03995	-8.31272	-16.7424
21.	2α,3β,23-trihydroxyolean-12-en-28-oic acid 28-O-β-D-glucopynoside	IMPHY008919	-1.85117	-15.0774	-21.7147
22.	Afrormosin	IMPHY004562	-1.78025	-20.562	-21.1698
23.	Arjunolone	IMPHY002418	-1.66583	-20.273	-24.6593
24.	Methyl oleanolate	IMPHY011461	-1.64274	-25.1935	-27.7402
25.	Friedelin	IMPHY011688	-1.48407	-18.2037	-17.7663
26.	Arachidic acid	IMPHY011394	-1.40582	-9.24243	-13.354
27.	Terminic acid	IMPHY008675	-1.19568	-18.6694	-25.0831
28.	Arjunone	IMPHY008708	-0.926594	-23.4387	-27.0636
29.	β-sitosterol	IMPHY014836	-0.827548	-17.1496	-20.2604
30.	Baicalein	IMPHY005607	-0.740031	-22.6366	-22.297
31.	Epigallocatechin	IMPHY011737	-0.460429	-13.1591	-27.4914
32.	Arjunic acid	IMPHY001431	1.02469	-18.4858	-18.6485

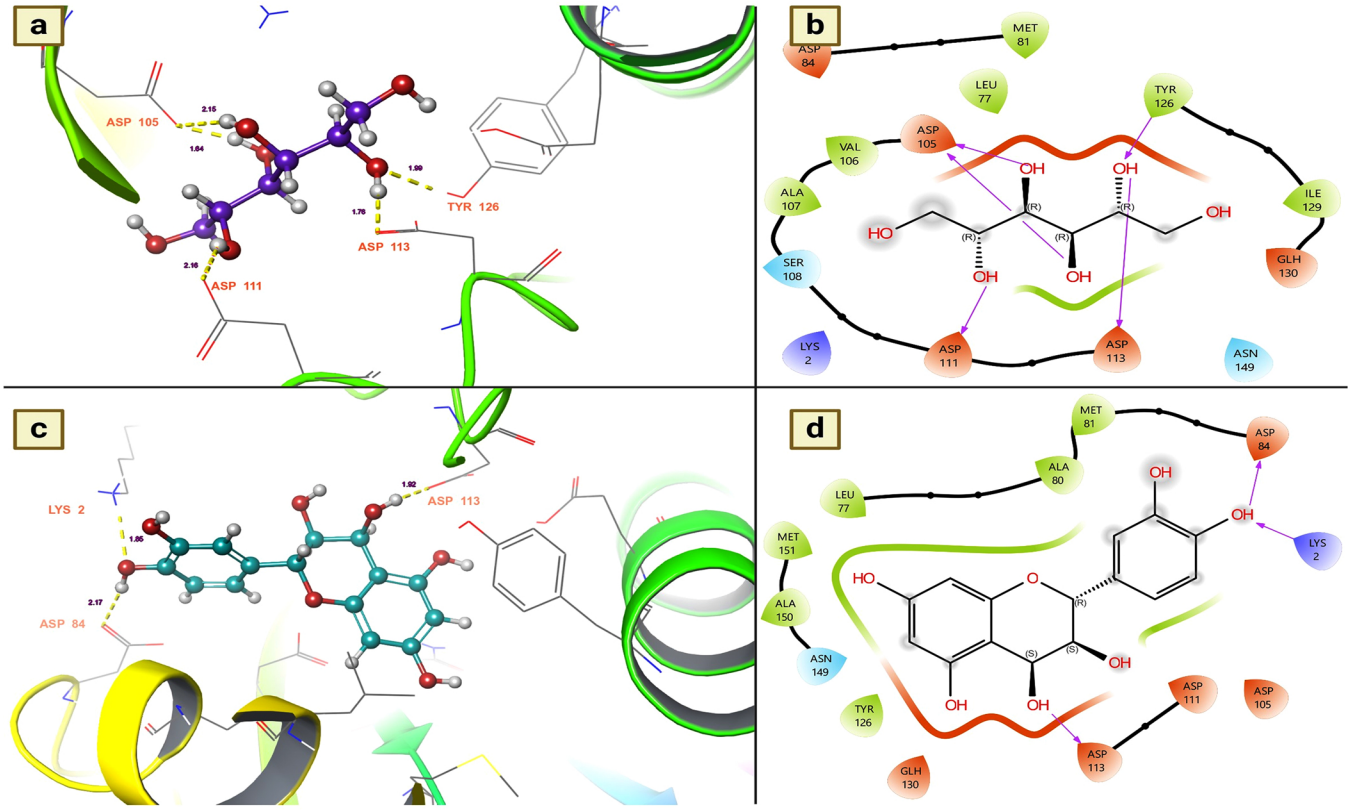

Fig. (4). (**a** and **b**). Mannitol shows the residues and hydrogen bond contacts with Arylalkylamine N-acetyltransferase 7; (**c** and **d**). Leucocianidol shows the residues and hydrogen bond contacts with Arylalkylamine N-acetyltransferase 7.

Table 6. Docking scores, Van Der Waals Forces and glide energies of *T. arjuna* chemical constituents against Odorant-binding protein 1 of *Aedes albopictus* (8BY4).

S.No.	Name of the Chemical Constituents	Phytochemical ID No. in IMPPAT 2.0	Docking Scores (Kcal/mol)	ΔGvdW	Glide Energy
1.	Mannitol	IMPHY004079	-5.78943	-9.82564	-18.9395
2.	Leucodelphidin	IMPHY012021	-5.69059	-1.37568	-7.53577
3.	Gallic acid	IMPHY011729	-4.4866	-7.43489	-19.8555
4.	(+)-Leucocyanidin	IMPHY011966	-4.0728	-18.5449	-20.8135
5.	8-Hydroxyhexadecanoic acid	IMPHY011699	-3.45731	-20.1668	-21.6849
6.	Catechol	IMPHY011885	-3.23348	-10.2046	-19.55
7.	Baicalein	IMPHY005607	-3.13506	-16.4068	-16.4195
8.	Arjunic acid	IMPHY001431	-3.13677	-21.3601	-27.7126
9.	Arjunolone	IMPHY002418	-3.11889	-14.9718	-22.8601
10.	Oxalic acid	IMPHY007450	-3.12999	-7.31149	-13.2972
11.	(+)-Gallocatechin	IMPHY011735	-2.94032	-17.1016	-21.0758
12.	Cerasidin	IMPHY002542	-2.8578	-17.8132	-23.907
13.	Epigallocatechin	IMPHY011737	-2.67806	-11.854	-14.2687
14.	Leucocianidol	IMPHY011611	-2.62756	-17.9488	-24.2757
15.	Afrormosin	IMPHY004562	-2.44469	-16.749	-19.7024
16.	Maslinic acid	IMPHY011970	-2.04159	-21.3541	-21.0542
17.	Arjunjenin	IMPHY012650	-2.03946	-18.9021	-22.2931
18.	Ellagic acid	IMPHY005537	-1.63761	-19.4892	-20.5654
19.	Methyl oleanolate	IMPHY011461	-1.3463	-21.8787	-21.4591
20.	Oleanolic acid	IMPHY011826	-1.23554	-16.8842	-19.3894

(Table 6) contd.....

S.No.	Name of the Chemical Constituents	Phytochemical ID No. in IMPPAT 2.0	Docking Scores (Kcal/mol)	ΔGvdW	Glide Energy
21.	Tomentosic acid	IMPHY012649	-1.16121	-14.4852	-13.407
22.	Stearate	IMPHY004097	-0.869246	-12.1962	-16.7029
23.	Arachidic acid	IMPHY011394	-0.395541	-14.1616	-16.0161
24.	Terminic acid	IMPHY008675	-0.323737	-20.8386	-22.2382

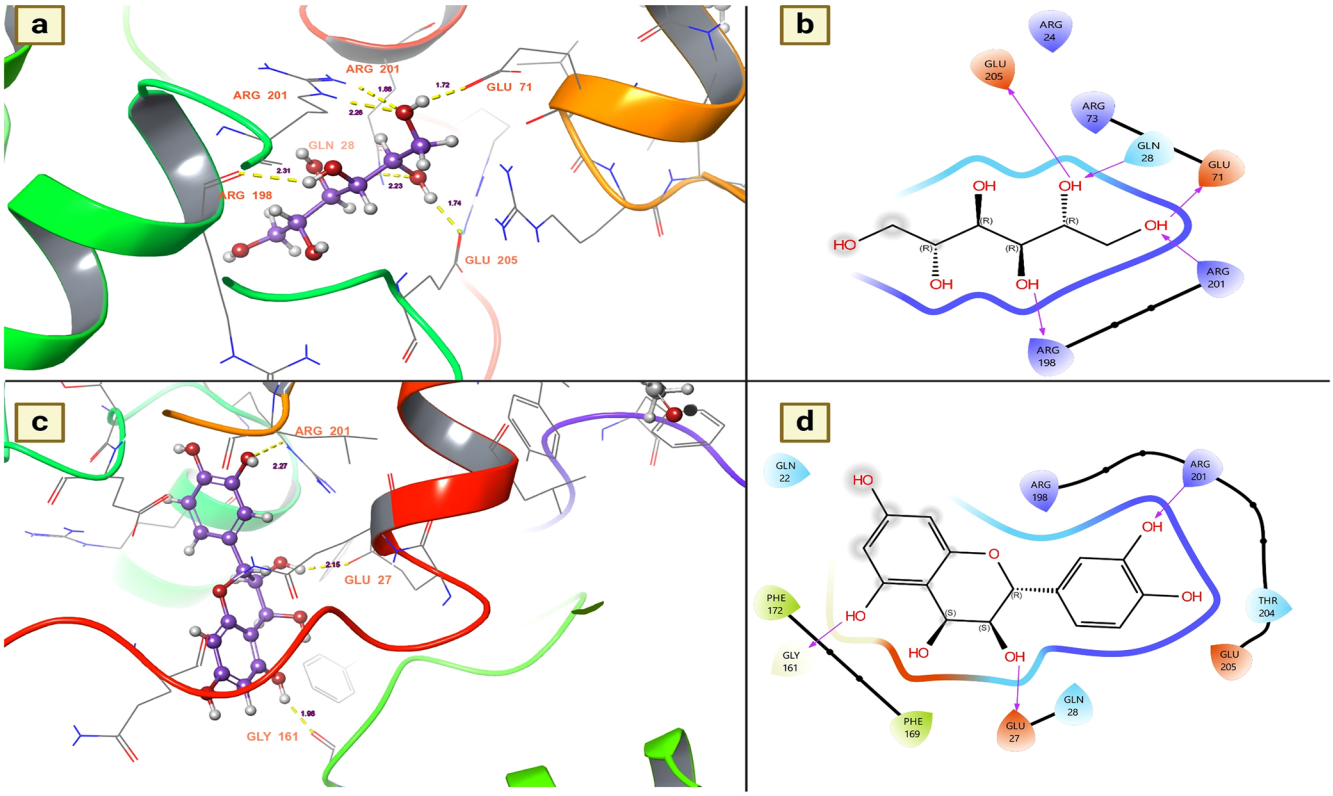

Fig. (5). (**a** and **b**). Mannitol shows the residues and hydrogen bond contacts with Juvenile hormone; **c** and **d**). Leucodelphidin shows the residues and hydrogen bond contacts with the Juvenile hormone.

3.3.4. Salivary Protein 34k2 from Aedes Albopictus (7TDR)

The salivary protein 34k2 plays a key role in blood feeding and the transmission of mosquito-borne diseases [35]. Furthermore, to facilitate blood feeding of the host, female mosquitoes secrete this protein upon bite, where it plays various roles, including blood clotting for easier suckling, dilation of blood vessels, and inhibition of the immune response [35]. The host also experiences allergic reactions such as itching, swelling, and redness at the feeding site. It also leads to the transmission of viruses to the host and modulates the immune response, favoring the survival of pathogens in the host. Considering its role in the transmission of the virus in the host, the present research investigated the effects of chemical components of *T. arjuna* on the denaturation efficiency of salivary proteins. The molecular docking studies showed that among the docked molecules, nearly 32 molecules were potential candidates for the denaturation of mosquito saliva protein 34k2 according to docking scores and binding affinities. Leucocianidol had a better docking score of -5.96534 Kcal/mol, followed by leucodelphidin (-5.87135 Kcal/mol), 2,3-(S)-hexahydro-xydiphenoyl-D-glucose (-5.74165 Kcal/mol), gallic acid (-4.70356 Kcal/mol), mannitol (-4.52336 Kcal/mol) and ellagic acid (-4.42596 Kcal/mol) (Table **5**). Moreover, to ascertain the binding affinities and provide insight into the denaturing efficacy of these complexes for salivary proteins, the effects of the docked complexes of leucocianidol and leucodelphidin on salivary proteins were explored. The assessment of the docked complex showed that leucocianidol has six contacts with this target. Of the six contacts, five are hydrogen bond contacts, and one is a pi-cation contact. Moreover, to denature the salivary protein, it selectively targets the following residues: GLU 182, ALA 178, LYS 217, ASP 220, and LYS 64. The results revealed that the distances of leucocianidol-target residue interactions were 2.16 for ALA 178, 2.13 for LYS 217, 1.77 and 2.07 for ASP 220, and 1.53 for GLU 182 (Fig. **6a** and **6b**). The hydrogen bond contacts of leucodelphinidin with residues are precisely shown in Fig. (**6c** and **6d**).

3.3.5. Odorant-binding Protein 1 from Aedes Albopictus (8BY4)

In mosquitoes, odorant binding protein 1 (OBPS 1) is involved in several processes, such as host-seeking, mating, and oviposition. However, by disrupting their olfactory-mediated behavior, the transmission of pathogens and their populations can be significantly reduced by repellent active ingredients of these OBPs1. Therefore, the present research aimed to identify mosquito OBP-1 repellents from *T. arjuna*. In this research, all chemical components of *T. arjuna* were found to disrupt the olfactory-mediated behavior of mosquitoes. Nearly 38 chemical components of *T. arjuna* were coupled with the OBPS 1 protein to determine their effect on OBPs1 in *A. albopictus*. Among the docked phytochemicals, 24 were found to be active at disrupting OBPs1. Of them, mannitol had a docking score of -5.78943 Kcal/mol with remarkable hydrogen bonding interactions (Table 6). Other chemical components, namely, leucodelphidin, gallic acid, and (+)-leucocyanidin, were found to have moderate docking scores of -5.69059 Kcal/mol, -4.4866 Kcal/mol and -4.0728 Kcal/mol, respectively (Table 6). The remaining molecules had the lowest docking scores, but they all had at least one contact with the OBPs-1 residues. The hydrogen bond contacts and the distances of the molecules showing notable docking metrics as possible candidates for OBPs-1 are shown in Fig. (7a-d).

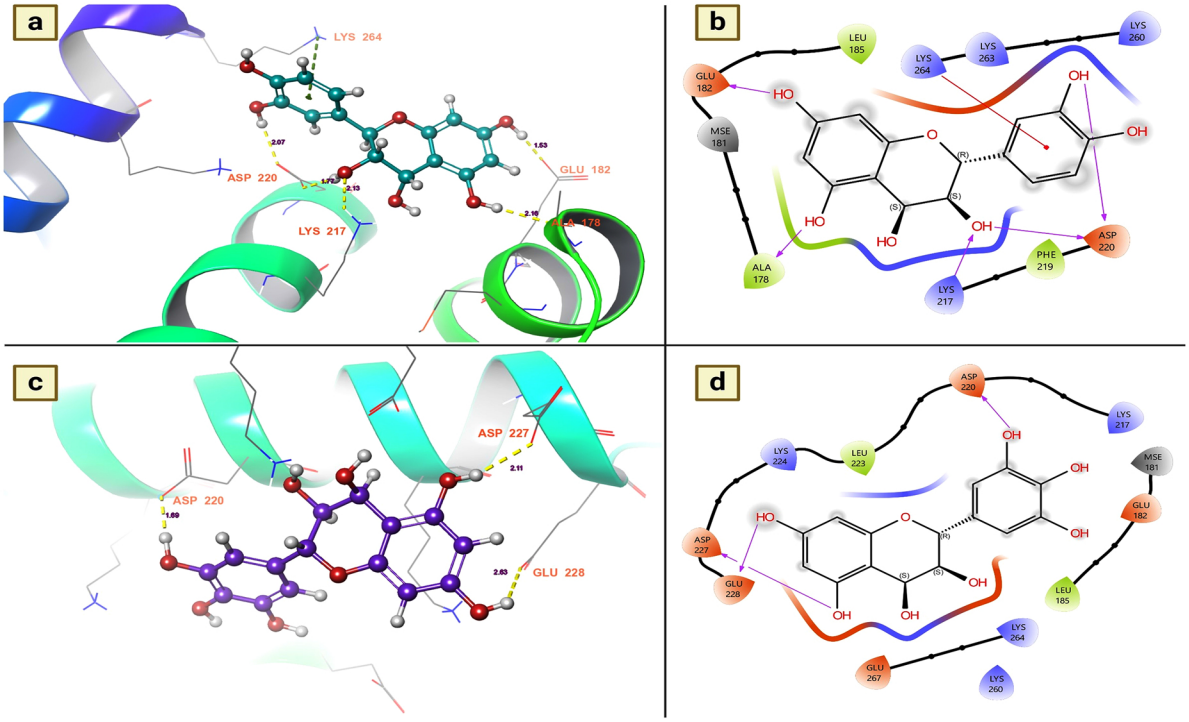

Fig. (6). (**a** and **b**). Leucocianidol shows the residues and hydrogen bond contacts with Salivary protein 34k2 of *Aedes albopictus*; (**c** and **d**). Leucodelphidin shows the residues and hydrogen bond contacts with the salivary protein 34k2 of *Aedes albopictus*.

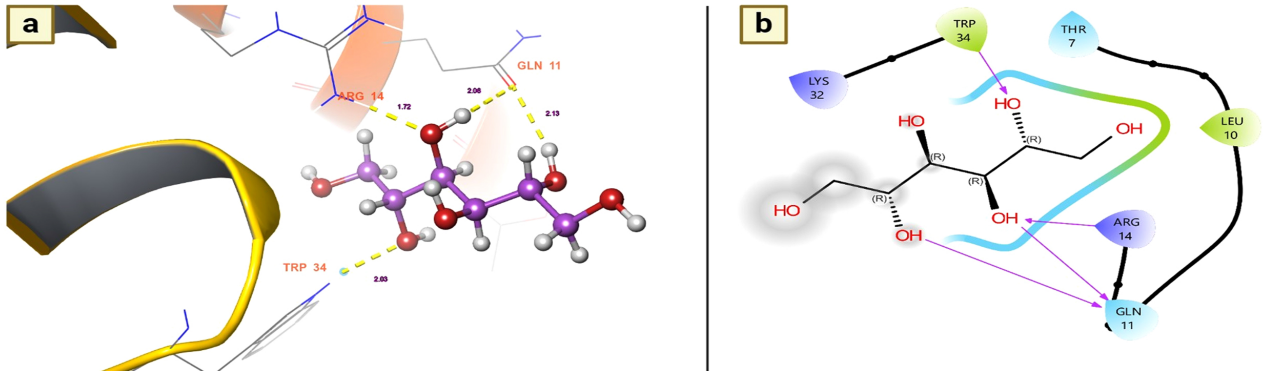

Fig. 7 contd.....

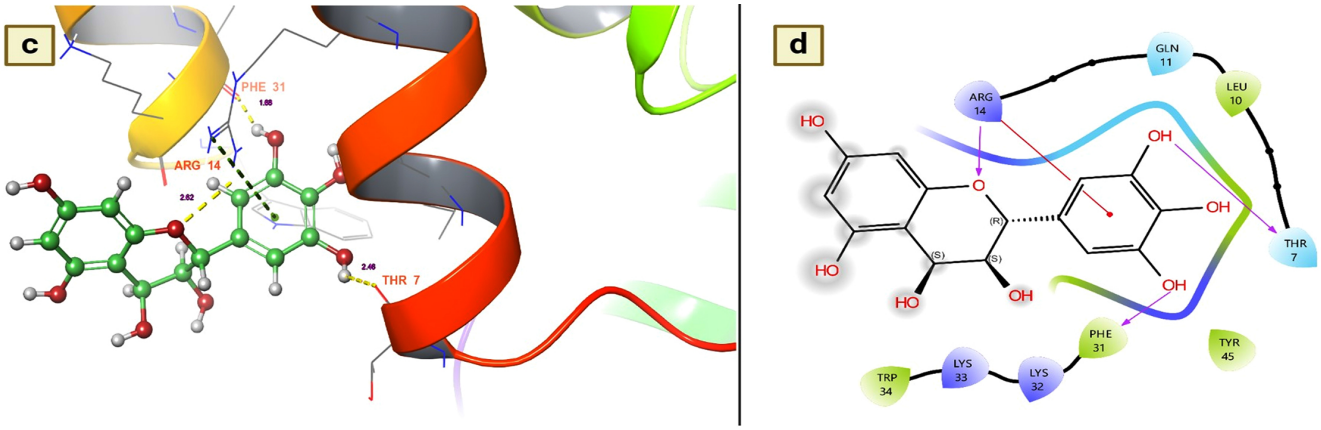

Fig. (7). (**a** and **b**). Mannitol shows the residues and hydrogen bond contacts with Odorant-binding protein 1 of *Aedes albopictus*; (**c** and **d**). Leucodelphidin shows the residues and hydrogen bond contacts with the Odorant-binding protein 1 of *Aedes albopictus*.

CONCLUSION

Green nanotechnology plays a key role in the pharmaceutical and agrochemical sectors because it enables the synthesis of the ideal product from metallic and nonmetallic components while removing dangerous elements during the synthesis process. It is believed to be more compatible and less expensive. However, less time is needed to synthesize AgNPs from natural sources such as plants and microorganisms. In this way, the present study achieved successful synthesis of AgNPs from the bark of *T. arjuna*. It has strong larvicidal effects on *A. albopictus* and *A. aegypti*. Based on the *in vitro* larvicidal effects of AgNPs, the phytochemicals of *T. arjuna* were investigated to evaluate their ability to reduce mosquito populations by targeting vital proteins. Through this *in silico* analysis, we observed that all the chemical compounds were revealed to have unique modes of action toward lowering vector populations and reducing disease transmission potencies. Thus, the current study indicated that these phytochemicals might serve as capping and reducing toxic element agents in the fabrication of silver nanoparticles for larvicidal purposes.

AUTHOR'S CONTRIBUTIONS

It is hereby acknowledged that all authors have accepted responsibility for the manuscript's content and consented to its submission. They have meticulously reviewed all results and unanimously approved the final version of the manuscript.

LIST OF ABBREVIATIONS

TABE = *Terminalia arjuna* bark extract

FT-IR = Fourier transform infrared spectroscopy

SEM = Scanning Electron Microscopy

XRD = X-ray diffraction analysis

EDX = EDX

FKBP = FK506-binding protein

ETHICS APPROVAL AND CONSENT TO PARTICIPATE

Not applicable.

HUMAN AND ANIMAL RIGHTS

Not applicable.

CONSENT FOR PUBLICATION

Not applicable.

AVAILABILITY OF DATA AND MATERIALS

The data supporting the findings of the article is available in the Protein databank and IMPAAT 2.0 at https://www.rcsb.org/ and https://cb.imsc.res.in/imppat/, reference number for proteins 2LPV, 4FD7, 5V13 and 7TDR.

FUNDING

None.

CONFLICT OF INTEREST

S Antony Ceasar is the Editorial Advisory Board member of The Open Biotechnology Journal.

ACKNOWLEDGEMENTS

Declared none.

REFERENCES

[1] WHO. Vector-borne Diseases. 2020. Available from: https://www.who.int/news-room/fact-sheets/detail/vector-borne-diseases

[2] Näslund J, Ahlm C, Islam K, Evander M, Bucht G, Lwande OW. Emerging mosquito-borne viruses linked to *Aedes aegypti* and *Aedes albopictus* : Global status and preventive strategies. Vector Borne Zoonotic Dis 2021; 21(10): 731-46. http://dx.doi.org/10.1089/vbz.2020.2762 PMID: 34424778

[3] Amarasinghe LD, Wickramarachchi PASR, Aberathna AAAU, Sithara WS, De Silva CR. Comparative study on larvicidal activity of green synthesized silver nanoparticles and Annona glabra (*Annonaceae*) aqueous extract to control Aedes aegypti and Aedes albopictus (*Diptera: Culicidae*). Heliyon 2020; 6(6): e04322.

http://dx.doi.org/10.1016/j.heliyon.2020.e04322 PMID: 32637705
[4] WHO. Disease Outbreak News. Dengue – Global situation 21. 2023. Available from: https://www.who.int/emergencies/disease-outbreak-news
[5] Yadav VK, Malik P, Khan AH, *et al*. Recent advances on properties and utility of nanomaterials generated from industrial and biological activities. Crystals 2021; 11(6): 634. http://dx.doi.org/10.3390/cryst11060634
[6] Yaqoob AA, Ahmad H, Parveen T, *et al*. Recent advances in metal decorated nanomaterials and their various biological applications: A review. Front Chem 2020; 8: 341. http://dx.doi.org/10.3389/fchem.2020.00341 PMID: 32509720
[7] Malik S, Muhammad K, Waheed Y. Emerging Applications of Nanotechnology in Healthcare and Medicine. Molecules 2023; 28(18): 6624. http://dx.doi.org/10.3390/molecules28186624 PMID: 37764400
[8] Nie D, Li J, Xie Q, *et al*. Nanoparticles: A Potential and Effective Method to Control Insect-Borne Diseases. Bioinorg Chem Appl 2023; 2023: 1-13. http://dx.doi.org/10.1155/2023/5898160 PMID: 37213220
[9] Kumar V, Sharma N, Saini R, *et al*. Therapeutic potential and industrial applications of *Terminalia arjuna* bark. J Ethnopharmacol 2023; 310: 116352. http://dx.doi.org/10.1016/j.jep.2023.116352 PMID: 36933876
[10] Ramasamy R, Surendran SN, Jude PJ, Dharshini S, Vinobaba M. Larval development of *Aedes aegypti* and *Aedes albopictus* in peri-urban brackish water and its implications for transmission of arboviral diseases. PLoS Negl Trop Dis 2011; 5(11): e1369. http://dx.doi.org/10.1371/journal.pntd.0001369 PMID: 22132243
[11] Guidelines for laboratory and field testing of mosquito larvicides. World Health Organization. 2005. Available from: https://www.who.int/publications/i/item/WHO-CDS-WHOPES-GCDPP-2005.13
[12] Venkadachalam R, Subramaniyan V, Palani M, Subramaniyan M, Srinivasan P, Raji M. Mosquito larvicidal and pupicidal activity of *Tephrosia purpurea* Linn. (Family: Fabaceae) and Bacillus sphaericus against, dengue vector, *Aedes aegypti*. Pharmacogn J 2017; 9(6): 737-42. http://dx.doi.org/10.5530/pj.2017.6.116
[13] Manimegalai T, Raguvaran K, Kalpana M, Maheswaran R. Green synthesis of silver nanoparticle using *Leonotis nepetifolia* and their toxicity against vector mosquitoes of *Aedes aegypti* and *Culex quinquefasciatus* and agricultural pests of *Spodoptera litura* and *Helicoverpa armigera*. Environ Sci Pollut Res Int 2020; 27(34): 43103-16. http://dx.doi.org/10.1007/s11356-020-10127-1 PMID: 32725570
[14] Vivek-Ananth RP, Mohanraj K, Sahoo AK, Samal A. IMPPAT 2.0: An Enhanced and Expanded Phytochemical Atlas of Indian Medicinal Plants. ACS Omega 2023; 8(9): 8827-45. http://dx.doi.org/10.1021/acsomega.3c00156 PMID: 36910986
[15] Vijayakumar S, Kasthuri G, Prabhu S, Manogar P, Parameswari N. Screening and identification of novel inhibitors against human 4-aminobutyrate-aminotransferase: A computational approach. Egypt J Basic Appl Sci 2018; 5(3): 210-9. http://dx.doi.org/10.1016/j.ejbas.2018.05.008
[16] Kalaimathi K, Thiyagarajan G, Vijayakumar S, *et al*. Molecular docking and network pharmacology-based approaches to explore the potential of terpenoids for Mycobacterium tuberculosis. Pharmacol Res - Mod Chin Med 2021; 1: 100002. http://dx.doi.org/10.1016/j.prmcm.2021.100002
[17] Ahmed Q, Gupta N, Kumar A, Nimesh S. Antibacterial efficacy of silver nanoparticles synthesized employing *Terminalia arjuna* bark extract. Artif Cells Nanomed Biotechnol 2017; 45(6): 1192-200. http://dx.doi.org/10.1080/21691401.2016.1215328 PMID: 27684206
[18] Singh P, Mijakovic I. Antibacterial effect of silver nanoparticles is stronger if the production host and the targeted pathogen are closely related. Biomedicines 2022; 10(3): 628. http://dx.doi.org/10.3390/biomedicines10030628 PMID: 35327429
[19] Zayed A, Robinson GE. Understanding the relationship between brain gene expression and social behavior: lessons from the honey bee. Annu Rev Genet 2012; 46(1): 591-615. http://dx.doi.org/10.1146/annurev-genet-110711-155517 PMID: 22994354
[20] Mollik SI, Alam RB, Islam MR. Significantly improved dielectric properties of bio-compatible starch/reduced graphene oxide nanocomposites. Synth Met 2021; 271: 116624. http://dx.doi.org/10.1016/j.synthmet.2020.116624
[21] Awad MA, Eid AM, Elsheikh TMY, *et al*. Mycosynthesis, characterization, and mosquitocidal activity of silver nanoparticles fabricated by *Aspergillus niger* strain. J Fungi 2022; 8(4): 396. http://dx.doi.org/10.3390/jof8040396 PMID: 35448627
[22] Parthiban E, Manivannan N, Ramanibai R, Mathivanan N. Green synthesis of silver-nanoparticles from *Annona reticulata* leaves aqueous extract and its mosquito larvicidal and anti-microbial activity on human pathogens. Biotechnol Rep 2019; 21: e00297. http://dx.doi.org/10.1016/j.btre.2018.e00297 PMID: 30581768
[23] Govindarajan M, Benelli G. A facile one-pot synthesis of eco-friendly nanoparticles using *Carissa carandas*: Ovicidal and larvicidal potential on malaria, dengue and filariasis mosquito vectors. J Cluster Sci 2017; 28(1): 15-36. http://dx.doi.org/10.1007/s10876-016-1035-6
[24] Govindarajan M, Benelli G. Facile biosynthesis of silver nanoparticles using *Barleria cristata*: mosquitocidal potential and biotoxicity on three non-target aquatic organisms. Parasitol Res 2016; 115(3): 925-35. http://dx.doi.org/10.1007/s00436-015-4817-0 PMID: 26555876
[25] Subramaniam J, Murugan K, Panneerselvam C, *et al*. Multipurpose effectiveness of *Couroupita guianensis*-synthesized gold nanoparticles: High antiplasmodial potential, field efficacy against malaria vectors and synergy with *Aplocheilus lineatus* predators. Environ Sci Pollut Res Int 2016; 23(8): 7543-58. http://dx.doi.org/10.1007/s11356-015-6007-0 PMID: 26732702
[26] Benelli G. Plant-mediated biosynthesis of nanoparticles as an emerging tool against mosquitoes of medical and veterinary importance: A review. Parasitol Res 2016; 115(1): 23-34. http://dx.doi.org/10.1007/s00436-015-4800-9 PMID: 26541154
[27] Tamilventhan A, Jayaprakash A. Larvicidal Activity of *Terminalia arjuna* Bark extracts on Dengue Fever Mosquito *Ades aegypti*. Res J Pharm Technol 2019; 12(1): 87-92. http://dx.doi.org/10.5958/0974-360X.2019.00017.9
[28] Subramaniam J, Murugan K, Panneerselvam C, *et al*. Eco-friendly control of malaria and arbovirus vectors using the mosquitofish *Gambusia affinis* and ultra-low dosages of *Mimusops elengi*-synthesized silver nanoparticles: towards an integrative approach? Environ Sci Pollut Res Int 2015; 22(24): 20067-83. http://dx.doi.org/10.1007/s11356-015-5253-5 PMID: 26300364
[29] Koul O. Phytochemicals and insect control: An antifeedant approach. Crit Rev Plant Sci 2008; 27(1): 1-24. http://dx.doi.org/10.1080/07352680802053908
[30] Rattan RS. Mechanism of action of insecticidal secondary metabolites of plant origin. Crop Prot 2010; 29(9): 913-20. http://dx.doi.org/10.1016/j.cropro.2010.05.008
[31] Chakraborty S, Britton M, Martínez-García PJ, Dandekar AM. Deep RNA-Seq profile reveals biodiversity, plant–microbe interactions and a large family of NBS-LRR resistance genes in walnut (*Juglans regia*) tissues. AMB Express 2016; 6(1): 12. http://dx.doi.org/10.1186/s13568-016-0182-3 PMID: 26883051
[32] Han Q, Robinson H, Ding H, Christensen BM, Li J. Evolution of insect arylalkylamine *N* -acetyltransferases: Structural evidence from the yellow fever mosquito, *Aedes aegypti*. Proc Natl Acad Sci USA 2012; 109(29): 11669-74. http://dx.doi.org/10.1073/pnas.1206828109 PMID: 22753468
[33] Kim IH, Pham V, Jablonka W, Goodman WG, Ribeiro JMC, Andersen JF. A mosquito hemolymph odorant-binding protein family member specifically binds juvenile hormone. J Biol Chem 2017; 292(37): 15329-39. http://dx.doi.org/10.1074/jbc.M117.802009 PMID: 28751377
[34] Arnoldi I, Mancini G, Fumagalli M, *et al*. A salivary factor binds a

cuticular protein and modulates biting by inducing morphological changes in the mosquito labrum. Curr Biol 2022; 32(16): 3493-3504.e11.
http://dx.doi.org/10.1016/j.cub.2022.06.049 PMID: 35835123

[35] Liggri PGV, Tsitsanou KE, Zographos SE. Crystal structure of Odorant Binding Protein 5 from Anopheles gambiae (AgamOBP5) with MPD (2-Methyl-2,4-pentanediol). 2023.
http://dx.doi.org/10.2210/pdb8BXU/pdb